Journal of Anatomy

J. Anat. (2018) **232**, pp686–698 doi: 10.1111/joa.12768

The clustering and morphology of chondrocytes in normal and mildly degenerate human femoral head cartilage studied by confocal laser scanning microscopy

Asima Karim,[1*] Anish K. Amin[2] and Andrew C. Hall[1]

[1]*Centre for Integrative Physiology, Deanery of Biomedical Sciences, University of Edinburgh, Edinburgh, UK*
[2]*Department of Orthopaedic and Trauma Surgery, University of Edinburgh, Edinburgh, UK*

Abstract

Chondrocytes are the major cell type present in hyaline cartilage and they play a crucial role in maintaining the mechanical resilience of the tissue through a balance of the synthesis and breakdown of extracellular matrix macromolecules. Histological assessment of cartilage suggests that articular chondrocytes *in situ* typically occur singly and demonstrate a rounded/elliptical morphology. However, there are suggestions that their grouping and fine shape is more complex and that these change with cartilage degeneration as occurs in osteoarthritis. In the present study we have used confocal laser scanning microscopy and fluorescently labelled *in situ* human chondrocytes and advanced imaging software to visualise chondrocyte clustering and detailed morphology within grade-0 (non-degenerate) and grade-1 (mildly degenerate) cartilage from human femoral heads. Graded human cartilage explants were incubated with 5-chloromethylfluorescein diacetate and propidium iodide to identify the morphology and viability, respectively, of *in situ* chondrocytes within superficial, mid- and deep zones. In grade-0 cartilage, the analysis of confocal microscope images showed that although the majority of chondrocytes were single and morphologically normal, clusters (i.e. three or more chondrocytes within the enclosed lacunar space) were occasionally observed in the superficial zone, and 15–25% of the cell population exhibited at least one cytoplasmic process of ~ 5 μm in length. With degeneration, cluster number increased (~ 50%) but not significantly; however, the number of cells/cluster ($P < 0.001$) and the percentage of cells forming clusters increased ($P = 0.0013$). In the superficial zone but not the mid- or deep zones, the volume of clusters and average volume of chondrocytes in clusters increased ($P < 0.001$ and $P < 0.05$, respectively). The percentage of chondrocytes with processes, the number of processes/cell and the length of processes/cell increased in the superficial zone of grade-1 cartilage ($P = 0.0098$, $P = 0.02$ and $P < 0.001$, respectively). Processes were categorised based on length (L0 – no cytoplasmic processes; L1 < 5 μm; 5 < L2 ≤ 10 μm; 10 < L3 ≤ 15 μm; L4 > 15 μm). With cartilage degeneration, for chondrocytes in all zones, there was a significant decrease ($P = 0.015$) in the percentage of chondrocytes with 'normal' morphology (i.e. L0), with no change in the percentage of cells with L1 processes; however, there were significant increases in the other categories. In grade-0 cartilage, chondrocyte clustering and morphological abnormalities occurred and with degeneration these were exacerbated, particularly in the superficial zone. Chondrocyte clustering and abnormal morphology are associated with aberrant matrix metabolism, suggesting that these early changes to chondrocyte properties may be associated with cartilage degeneration.

Key words: cartilage; chondrocyte clustering; chondrocyte morphology; confocal laser scanning microscopy; cytoplasmic processes; femoral head.

Correspondence
Andrew C. Hall, Centre for Integrative Physiology, Deanery of Biomedical Sciences, Hugh Robson Building, George Square, Edinburgh EH8 9XD, Scotland, UK. T: + 44 (0)131 6503263; F: + 44 (0)131 6502872; E: a.hall@ed.ac.uk

**Current address: Department of Physiology & Cell Biology, University of Health Sciences, Lahore, Pakistan*

Accepted for publication *30 November 2017*
Article published online *28 December 2017*

Introduction

Articular cartilage has a highly specialised structure which imparts remarkable load-bearing properties over many decades. Chondrocytes are the major cell type and are primarily responsible for the maintenance of the resilient extracellular matrix, and a small but distinct population of cartilage-derived stem/progenitor cells has also been reported (Dowthwaite et al. 2004). Cartilage properties vary with depth from the superficial zone through to the mid-zone and finally the deep zone. These zones and their resident chondrocytes have different biomechanical (Chen et al. 2001; Vanderploeg et al. 2008) and metabolic properties (Aydelotte & Kuettner, 1988; Wong et al. 1996; Simpkin et al. 2007). From histological studies, the topographical arrangement and morphology of chondrocytes within the zones of normal (non-degenerate) articular cartilage have been described (Hunziker, 1992). Although there are differences between animal species and joints, in non-degenerate cartilage, cell shape and distribution vary with depth. Superficial zone chondrocytes tend to have an elliptical, flattened appearance lying parallel to the surface. Mid-zone chondrocytes are spheroidal and randomly arranged, whereas deep zone chondrocytes are almost all rounded and aligned in perpendicular columns. These adaptations are probably related to the prevailing biomechanical forces, which range from predominantly shearing/tensional stresses in the superficial zone, to mainly compressional forces in the deep zone (Grodzinsky et al. 2000). Chondrocyte clustering is also a property of some normal cartilages. For example, in the superficial zone of human ankle cartilage, horizontal cell clustering (described as 'strings') parallel to the surface occurs (Schumacher et al. 2002; Rolauffs et al. 2010). However, clustering is more usually associated with degenerative joint disease (also known as osteoarthritis) where increased cell number and size are often localised near surface fissures (Lotz et al. 2010). Associated with cartilage degeneration, there are substantial changes to the cells and matrix, leading to a loss in zonal characteristics (Buckwalter & Mankin, 1997) as well as increased chondrocyte proliferation (Rothwell & Bentley, 1973; Lotz et al. 2010; Rolauffs et al. 2010), possibly resulting from changes to the chondron microenvironment (Poole et al. 1991).

There is increasing evidence that human chondrocyte morphology is more varied than these 'classical' elliptical/spheroidal forms (Bush & Hall, 2003; Murray et al. 2010). Advances have been made in the visualisation of living *in situ* chondrocyte morphology using fluorescent dyes and confocal scanning laser microscopy (Bush & Hall, 2003). Approximately half of the chondrocytes within macroscopically normal (non-degenerate, aged) human tibial plateau cartilage, have cytoplasmic processes extending beyond the pericellular matrix/lacuna into the inter-territorial matrix (Bush & Hall, 2003). Similar abnormal 'fibroblastic-like' chondrocytes have been observed in human femoral head cartilage overlaid with pannus (Holloway et al. 2004) and in histological/electron microscopical studies of normal and fibrillated human knee cartilage (Kouri et al. 1998; Tesche & Miosge, 2005). The processes are not related to the chondrocyte primary cilium (McGlashen et al. 2008).

The development of abnormal chondrocyte morphology in non-degenerate cartilage could be important as there is a close relationship between the actin cytoskeleton, a major controller of chondrocyte morphology (Blaine, 2009), and chondrocyte differentiation (Mallein-Gerin et al. 1991; Rottmar et al. 2014). Chondrocytes are phenotypically unstable and cytoskeletal integrity can affect matrix metabolism and thus, potentially, cartilage resilience. For example, during chondrocyte de-differentiation, expression of cartilage markers of the transcription factor SOX9, and production of cartilage-specific matrix molecules (aggrecan, collagen Type II) are reduced, whereas synthesis of fibro-cartilagenous constituents (e.g. Type I collagen) is increased (Stokes et al. 2001; Woods et al. 2007). However, de-differentiation is reversible, as chondrocytes with 'fibroblastic' morphology re-express the chondrogenic phenotype upon restoration of a spheroidal shape, e.g. in agarose culture (Benya & Shaffer, 1982) or with cytoskeletal disruption (Blaine, 2009).

To determine whether there is a relationship between changes to chondrocyte clustering and morphology from classical (elliptical/spheroidal) forms to abnormal shapes/clusters and the degree of cartilage degeneration, we have classified clusters and morphology of *in situ* chondrocytes using a quantitative approach. We have obtained osteochondral explants from normal (non-degenerate; grade-0) and mildly degenerate (grade-1) human femoral head cartilage and then incubated them with 5-chloromethylfluorescein diacetate, a cytoplasmic dye which fluoresces green within chondrocytes, and propidium iodide, which fluoresces red and identifies dead chondrocytes. Using confocal scanning laser microscopy and imaging of relatively unperturbed *in situ* chondrocytes in standardised regions of interest in the superficial, mid- and deep zones of grade-0 and grade-1 cartilage, we have then determined (1) the average number of clusters, (2) the average number of cells per cluster, (3) the percentage of cells present in clusters, (4) the average volume of clusters (in μm^3) and (5) the average volume of individual cells in a cluster (in μm^3). For chondrocyte morphology, we have measured (1) the percentage of cells with cytoplasmic processes, (2) the number of processes per cell and (3) the average length of cytoplasmic processes (in μm). The results revealed the marked heterogeneity of human chondrocyte grouping and morphology, particularly within normal (non-degenerate) cartilage, where small chondrocyte clusters and short cytoplasmic processes were identified. Furthermore, there were marked changes to chondrocyte clusters and morphology with progression of cartilage degeneration from grade-0 (non-degenerate) to grade-1 (mildly degenerate).

Materials and methods

Human femoral head articular cartilage

Femoral heads were obtained with Ethical Permission (Tissue Governance, National Health Service, Lothian) from 11 patients undergoing surgery only for hip hemiarthroplasty due to fractured neck of femur: eight females, three males, 77.8 ± 5.8 years [mean ± confidence intervals (95%); range 65–89 years]; grade-0 78.9 ± 7.8 years, range 64–89 years; grade-1 76.6 ± 9.2 years, range 65–89 years. Heads were immediately transferred to Dulbecco's modified Eagle's medium (pH 7.4) supplemented with penicillin/streptomycin (100 units mL^{-1} and 100 μg mL^{-1}, respectively; Invitrogen, Paisley, UK). Throughout, care was taken to avoid tissue injury during handling (Huntley et al. 2005) or dehydration (Paterson et al. 2015), with experiments being performed within 10 h of surgery.

Cartilage grading

Cartilage was assessed by a clinician (A.K.A.) and a biomedical scientist (A.K.) using Osteoarthritis Research Society International (OARSI) criteria (Pritzker et al. 2006). Visually, grade-0 cartilage was smooth and shiny with no roughness/fibrillations, whereas grade-1 cartilage areas were discoloured and appeared rough with occasional superficial splitting. The surface roughness of explants was visualised by adjusting the brightness/contrast of the confocal laser scanning microscope images, further assisting cartilage grading (Fig. 1). For most of the femoral heads the cartilage was non-degenerate (grade-0) over > 75% of the surface. However, in some femoral heads, there were relatively small areas (covering approximately 25%) of grade-1 cartilage, present mostly at two locations around the fovea: parafoveal posterior and parafoveal inferior. Pannus (Shibakawa et al. 2003) was not observed on any joints.

Cartilage harvesting and fluorescent labelling

Osteochondral explants making up the full cartilage thickness with subchondral bone were harvested from graded areas. Explants were trimmed to ~ 5 × 5 mm using fresh scalpel blades to minimise chondrocyte death (Amin et al. 2008) and stored in Dulbecco's modified Eagle's medium. They were then incubated with 5-chloromethylfluorescein diacetate and propidium iodide (12.5 and 10 μM, respectively; 2 h; 21 °C) to label living (green) and dead (red) cells, respectively (Amin et al. 2008). Explants were washed in phosphate-buffered saline, fixed (formaldehyde 4% v/v; Fisher Scientific, Leicestershire, UK) and mounted for imaging.

Confocal laser scanning microscopy

Fluorescently labelled *in situ* chondrocytes were imaged using a Zeiss Axioskop LSM510 (Carl Zeiss, Welwyn Garden City, UK) (E_x = 488 nm and 543 nm for 5-chloromethylfluorescein diacetate and propidium iodide, and E_m = 505–530 and 650 nm, respectively). Cartilage appearance, chondrocyte viability, thickness and delineation of zones were initially evaluated at low power (×10 dry; numerical aperture = 0.3). Chondrocyte morphology/clustering was determined at high power (×40; numerical aperture = 0.8). Sequential *z*-stack images in axial and coronal planes to 100 μm for low, and 50 μm for high power magnification with intervals of 5 and 1 μm, respectively (frame size 1024 × 1024 pixels) were obtained (Amin et al. 2008).

Demarcation of cartilage zones

Criteria (Hembree et al. 2007) were applied which depended on the morphology and orientation of chondrocytes visualised with low-power (×10) images. Superficial zone chondrocytes tended to be ellipsoidal, with their long axis orientation parallel to the cartilage surface and made up ~ 10% of the cartilage thickness. Mid-zone chondrocytes tended to be spheroidal, more randomly orientated, and made up ~ 60% of the cartilage thickness. Deep zone chondrocytes were spheroidal, frequently in columns preferentially oriented perpendicular to the tidemark with subchondral bone, and made up ~ 30% of the tissue thickness.

Morphological analysis of *in situ* chondrocytes

Quantitative data regarding chondrocyte clusters and cytoplasmic processes were obtained by three-dimensional analysis of high power (×40) images utilising Volocity™ (Improvision, Coventry, UK) (Amin et al. 2008). Human chondrocytes occur singly, in pairs or clusters within a lacuna, with a cluster comprising three or more chondrocytes within the enclosed lacunar space (Rolauffs et al. 2010). The volume of clusters was measured using Volocity™ against calibrated fluorescent beads (Fluoresbrite™, Polyscience, Warrington, UK) (Bush & Hall, 2001). The number of cells/cluster was counted manually; however, it was not possible to measure the volume of individual chondrocytes accurately because cells were frequently touching and identifying the membrane edge was unreliable. Average cell volume in a cluster was determined as: cell volume in a cluster (μm^3) = [total volume of cluster (μm^3)]/(total number of cells in cluster). The total number of chondrocytes within the region of interest (dimensions; *x*, *y*, *z* of 228, 228, 50 μm, respectively) were counted, and the percentage of cells forming clusters calculated as: % cells in a cluster = 100 × (number of cells forming clusters/total number of cells)%.

Spheroidal/elliptical chondrocytes with no cytoplasmic processes were considered to have 'normal' morphology. The morphology of chondrocytes with one or more cytoplasmic processes was described as being 'abnormal', although it should be noted that this term referred only to the shape of the cells and not to any other physiological or pathological changes (Bush & Hall, 2003). The percentage of abnormal chondrocytes was calculated as: abnormal chondrocytes (%) = 100 × (number of abnormal cells)/(number of normal + abnormal cells)%. The length of cytoplasmic processes (in μm) was determined by tracing in three dimensions from their initiation at the cell body to their end. Cells with/without processes were further categorised into five groups based on their length (L): (L0 no processes present, L1 < 5 μm, 5 < L2 ≤ 10 μm, 10 < L3 ≤ 15 μm and L4 > 15 μm) permitting a more detailed quantitative comparison between cells in the different zones. The percentage of chondrocytes with cytoplasmic processes in each category was calculated as: chondrocytes in length category (L1–4) (%) = 100 × (number of cells with specific length category (L1-4))/total number of cells with processes)%. The number of cells was counted in the specified regions of interest and cell density calculated as: cell density (number of cells $mm^{-3} \times 10^3$) = total no. of cells labelled with 5-chloromethylfluorescein diacetate and propidium iodide/volume of cartilage imaged (μm^3).

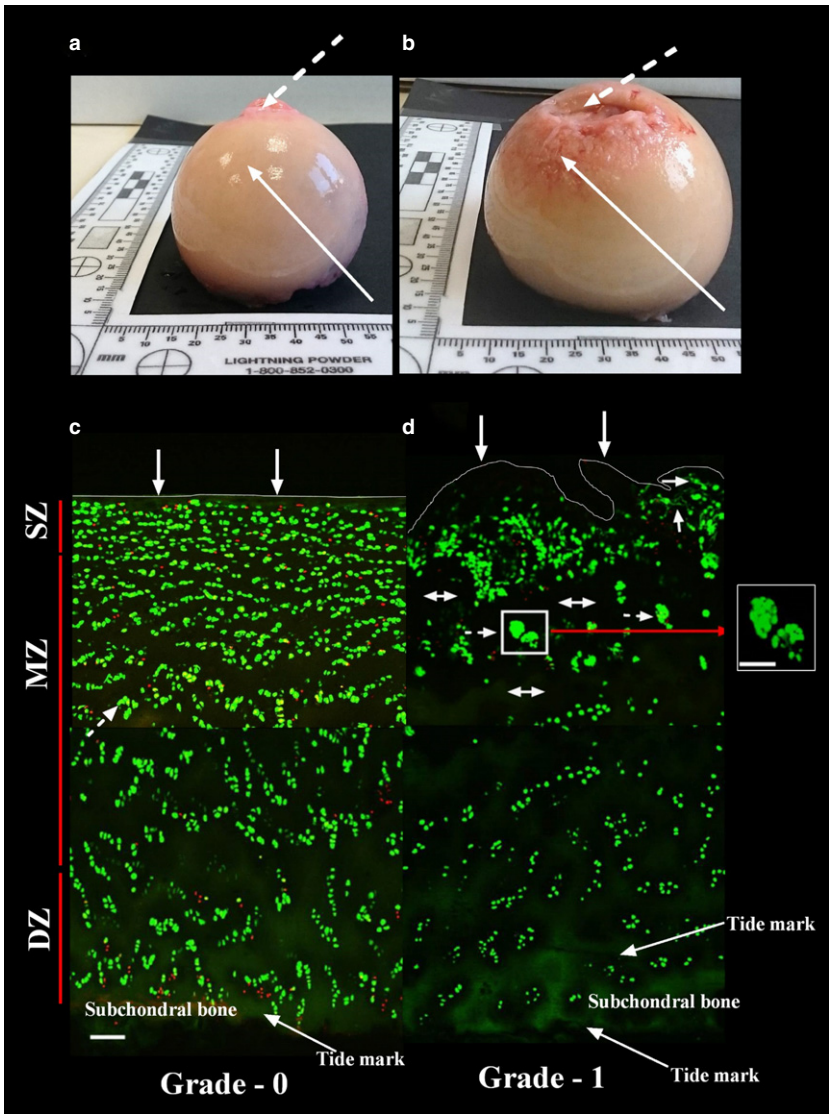

Fig. 1 Macroscopic and microscopic overview of grade-0 and grade-1 human femoral articular cartilage. The upper two panels show examples of the macroscopic appearance of human femoral heads obtained from (a) a male patient (64 years) and (b) a female patient (85 years) with cartilage graded at the solid arrows as grade-0 and grade-1, respectively. The broken arrows indicate the fovea. Macroscopic grading of cartilage was initially performed using Osteoarthritis Research Society International criteria, followed by a microscopic grading which was determined by studying the cartilage surface of the explants to be imaged (see Materials and methods). The lower two panels show representative confocal scanning laser microscopy low power (×10) images of 5-chloromethylfluorescein diacetate- and propidium iodide-labelled chondrocytes viewed in the coronal plane in (c) grade-0 and (d) grade-1 cartilage. The approximate thicknesses of the zones (SZ = superficial zone; MZ = mid-zone; DZ = deep zone) are shown. Grade-0 cartilage showed a smooth regular surface with minor morphological changes to chondrocytes, whereas grade-1 displayed obvious surface discontinuity and erosions with chondrocyte clustering. Cytoplasmic processes of chondrocytes could not be visualised at this magnification. Solid arrows indicate smooth and rough surfaces of grade-0 and grade-1 cartilage, respectively, double-headed arrows indicate areas of hypo-cellularity, and broken arrows indicate examples of chondrocyte clusters present in grade-1 cartilage. Scale bars: 100 μm (a-d) and 50 μm (inset).

Data presentation and analysis

Data were presented as mean ± confidence intervals (95%) for [*N*(*n*)], with *N* representing the number of cartilage samples from separate donors and *n* the number of chondrocytes. Histograms and statistical tests were performed using GraphPad Prism 6 (GraphPad, La Jolla, CA, USA). Student's *t*-tests were used to compare data between grade-0 and grade-1 cartilage. One-way analysis of variance with Tukey's post-hoc test were applied for comparison between and within groups. Significance was accepted when $P < 0.05$. An asterisk (*) indicated a significant difference according to Student's *t*-tests and the hash symbol (#) indicated a significant difference by analysis of variance. Single, double and triple symbols indicated significance for $P < 0.05$, 0.01 and 0.001, respectively, with actual values given where appropriate in the text.

Results

Thickness and zones of human femoral head cartilage

Full-depth grade-0 cartilage was 1554 ± 66 μm ($N = 6$; range 1398–1648 μm; mean ± confidence intervals). Thickness when measured at four different areas (parafoveal anterior, parafoveal posterior, parafoveal superior and parafoveal inferior) was not different between these areas ($P > 0.05$) [parafoveal anterior (1519 ± 253 μm; $N = 3$), parafoveal posterior (1559 ± 403 μm; $N = 2$), parafoveal superior (1618 ± 40 μm; $N = 3$) and parafoveal inferior (1305 ± 41 μm; $N = 3$)]. Grade-0 cartilage surface was smooth and regular; however, grade-1 cartilage was clearly uneven (Fig. 1c,d). Grade-1 cartilage thickness measurements were difficult because of the irregular surface and cartilage-bone interface. However, the thickness of grade-1 cartilage was 1512 ± 85 μm ($N = 5$; range 1335–1665 μm), and similar to grade-0 cartilage.

The superfical, mid- and deep zones were defined as 10, 60 and 30%, respectively, of the overall cartilage depth (Hembree et al. 2007) corresponding to zones of approximate thicknesses: superficial zone, 155 μm; mid-zone 155–932 μm; deep zone 466 μm (Fig. 1, grade-0). Coronal images of grade-0 and grade-1 cartilage showed differences in chondrocyte orientation/morphology between zones. In grade-0 cartilage, zones could be demarcated reasonably accurately from the characteristic pattern of chondrocytes with depth. However, in grade-1 cartilage, chondrocyte arrangement was disturbed and zone identification unclear. In the superficial zone, clusters were infrequent in grade-0 but clearly identified in grade-1 cartilage (Fig. 1c,d). While these images illustrated important features of grade-0 and grade-1 cartilage, high power magnification was essential to visualise fine morphological features of chondrocytes in non-degenerate cartilage and any changes in grade-1 cartilage.

Overview of grade-0 and grade-1 human femoral head cartilage (axial views)

Images taken distant from any cut edge (Fig. 2a-d) represented chondrocyte morphology within relatively unperturbed cartilage. In grade-0 cartilage, chondrocytes were mostly spheroidal/elliptical, with few hypo-cellular areas (Fig. 2a). However, in grade-1, heterogeneity of chondrocyte morphology and absence of cells were evident (Fig. 2b). Few propidium iodide-labelled cells were observed in either grade (Fig. 2), suggesting minimal chondrocyte death associated with cartilage preparation. In grade-0 cartilage, some cells had cytoplasmic processes (Fig. 2c). In grade-1, however, many chondrocytes exhibited abnormal morphology/processes, and some clustering was evident (Fig. 2d). In grade-0 cartilage, processes were short (≤ 5 μm) and 64 ± 4% [$N(n) = 11(1178)$] were curled within the lacunar space, with approximately 36 ± 4% having straight processes. In grade-1, processes were longer (> 5 μm) with 53 ± 5% and 46 ± 5% [$N(n) = 5$ (563)] curled and straight, respectively, suggesting that with cartilage degeneration, lacunae were disrupted and processes extended into the inter-territorial matrix (Fig. 2c,d). Cell density was not different between zones: superficial zone 27.8 ± 1.5 and 28.6 ± 3.0 cells $mm^{-3} \times 10^3$, mid-zone 13.8 ± 1.1 and 13.6 ± 2.0 cells $mm^{-3} \times 10^3$ and deep zone (11.9 ± 1.0 and 12.8 ± 1.6 cells $mm^{-3} \times 10^3$ for grade-0 and grade-1, respectively, $N = 5$ for each). However, clustering in grade-1 was extensive, potentially compensating for chondrocyte loss with degeneration.

Chondrocyte properties in grade-0 and grade-1 human articular cartilage (coronal views)

High power (×40) images (Fig. 3) showed increased heterogeneity of chondrocyte morphology in grade-1 compared with grade-0 cartilage. Although the majority of chondrocytes in grade-0 exhibited normal morphology, cells with fine cytoplasmic processes were routinely observed. Clustering was infrequent but, when present, there were only a few chondrocytes/cluster. However, in grade-1, many large clusters involving numerous chondrocytes/cluster were observed, with many individual chondrocytes exhibiting cytoplasmic processes. These changes in grade-1 cartilage appeared greatest in the superficial zone, and were less marked in the mid-zone and least marked in the deep zone (Fig. 3).

Chondrocyte cluster formation

Number of clusters, number of chondrocytes/cluster and percentage of cells forming clusters. Chondrocyte clustering was occasionally observed in grade-0 (Fig. 1c) and appeared confined to the superfical zone with only a few cells/cluster. However, clustering was routinely observed in grade-1 cartilage (Fig. 4b). In both grades, the number of clusters was higher in the superficial zone than in the deep zone (Fig. 4a,b; $P < 0.001$ and $P < 0.05$, respectively). Although the average number of clusters was ~ 50% greater in the superficial zone of grade-1 compared with grade-0, this was not significant ($P = 0.24$). In grade-0 cartilage, the average number of cells/cluster (3.6 ± 0.4) was the same in all zones (Fig. 4c; $P > 0.05$). Comparing the superficial zone in grade-0 and grade-1, there was an increase to 9.8 ± 1.7 cells/cluster (Fig. 4d; $P = 0.0002$) in the latter, as well as an increase in the percentage of superficial zone chondrocytes forming clusters (15.6 ± 3.0 to 61 ± 10.5%; Fig. 4e,f; $P < 0.001$). However, although 25% of the mid-zone chondrocytes formed clusters in

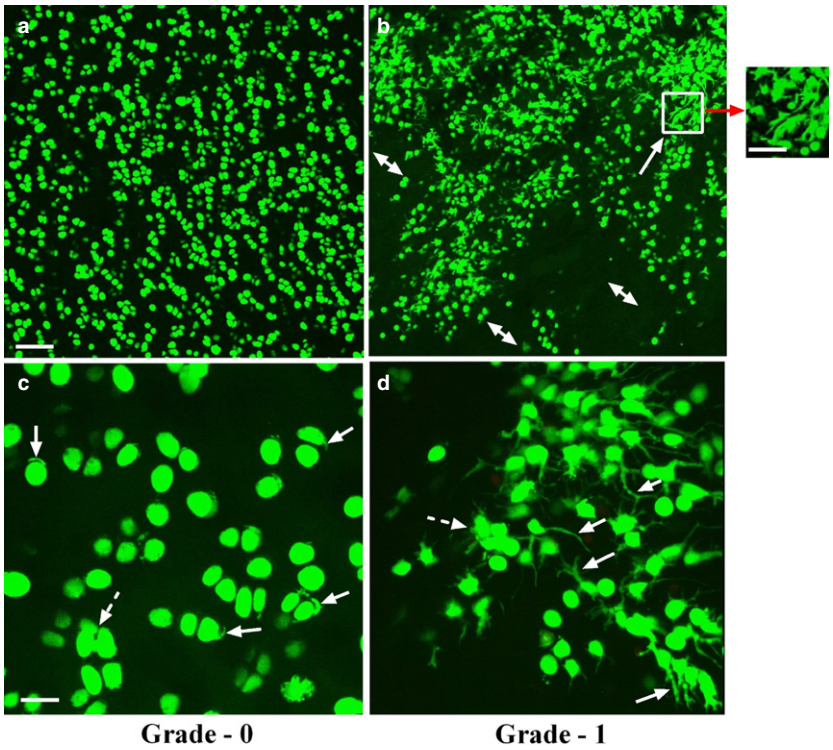

Fig. 2 Low and high power axial confocal laser scanning microscope reconstructed images of chondrocytes within grade-0 and grade-1 human femoral head articular cartilage. Representative examples of confocal laser scanning microscope images at low magnification (×10) 5-chloromethylfluorescein diacetate- and propidium iodide-labelled chondrocytes (live and dead cells, respectively) in human (a) grade-0 and (b) grade-1 cartilage explants. At low magnification, chondrocyte morphology and distribution in grade-0 cartilage appeared relatively normal; however, in mildly degenerate (grade-1) samples, evidence of chondrocyte clustering (solid arrow) and areas of hypocellularity were present (double-headed arrows). Scale bars: 100 μm (a,b) and 50 μm (inset). At high magnification (panel c) (×40), the majority of chondrocytes in grade-0 cartilage demonstrated normal morphology, but some cells with short, often curled, cytoplasmic processes were present (solid arrows) with infrequent clustering of chondrocytes (≥ 3 cells; broken arrow). In grade-1 cartilage (d), many cells possessed cytoplasmic processes of varying length (solid arrows) and number, and there was extensive clustering (inset in b, and broken arrow in d). Note that there were no propidium iodide-labelled chondrocytes detected in these images even though this fluorescent indicator was present. Scale bars: 25 μm (c,d).

grade-1 (Fig. 4f) compared with grade-0 cartilage (~ 8%; Fig. 4e), this was not significant. In the deep zone, the number of chondrocytes forming clusters was negligible in both grades (Fig. 4e,f). When comparing all zones, there was also no significant difference in the average number of clusters (Fig. 4b), but there was in the average number of cells/cluster (Fig. 4d; $P = 0.0001$), and in the percentage of chondrocytes forming clusters (Fig. 4f; $P = 0.0013$). This suggests that although the number of clusters was not different between the cartilage grades, more chondrocytes were involved in cluster formation.

Volume of clusters and average volume of chondrocytes within clusters. Average chondrocyte volume in a cluster in grade-0 cartilage was ~ 5000 μm^3 and was similar in all zones (Fig. 4g). However, only in the superficial zone of grade-1 did volume increase significantly, reaching > 15 000 μm^3 (Fig. 4h; $P < 0.001$) with no significant change in the mid- or deep zone. The average volume of single cells in superficial zone clusters of grade-1 cartilage was ~ 21% greater than that in grade-0 cartilage (Fig. 4j; $P = 0.04$). Although the data for the volume of clusters and volume of individual cells in clusters in the mid- and deep zone of both cartilage grades referred to a relatively small number of clusters, there were no significant differences between zones. Although the volume of individual superficial zone chondrocytes in clusters increased with cartilage degeneration, when the average volume of chondrocytes in clusters in all zones were compared, there was no significant difference between grades (Fig. 4i,j). Furthermore, although the number of clusters did not change, there was a marked increase in the number of cells/cluster, suggesting proliferation was the mechanism for increased cluster size, rather than chondrocyte swelling.

Fine chondrocyte morphology

Percentage of abnormal chondrocytes. Chondrocytes were categorised into five groups based on the length (L) of cytoplasmic processes: (L0 no processes

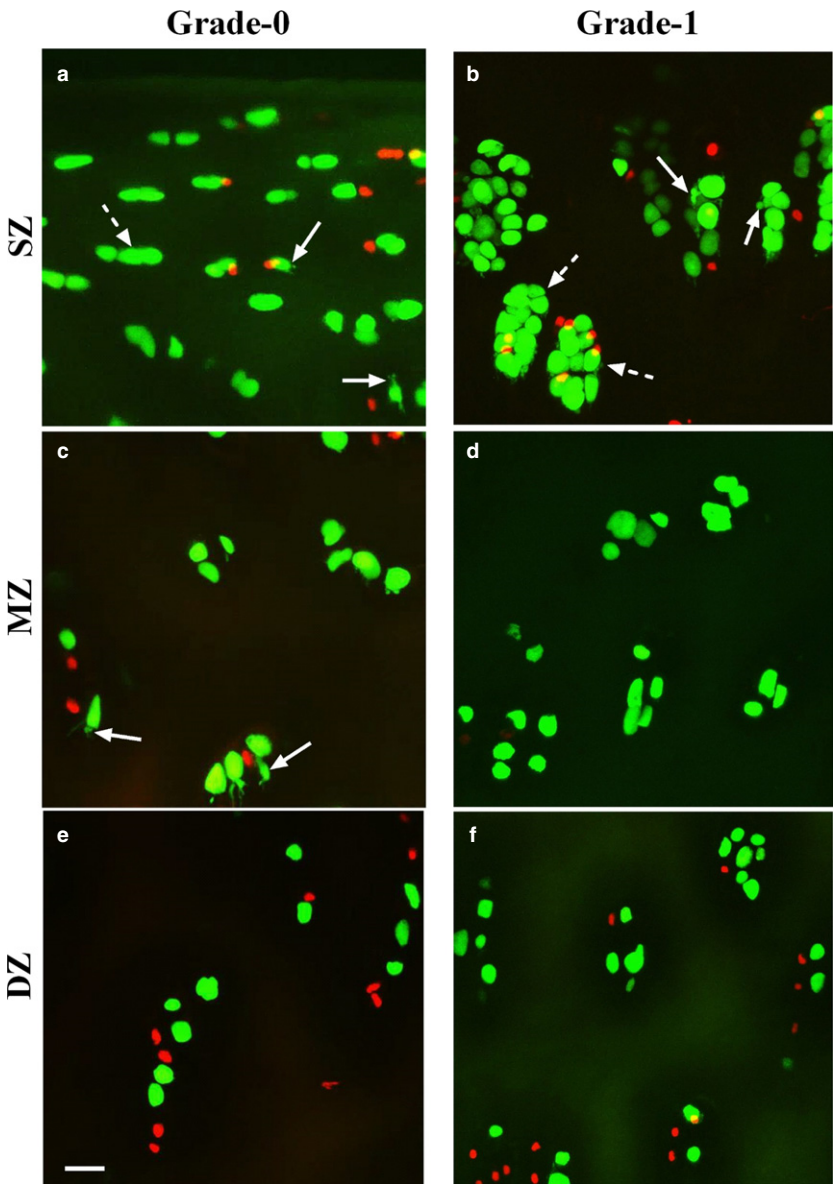

Fig. 3 High power coronal confocal laser scanning microscope reconstructed images of chondrocytes within grade-0 and grade-1 human femoral articular cartilage. High power (×40) coronal images of fluorescently labelled chondrocytes (5-chloromethylfluorescein diacetate and propidium iodide for live and dead cells, respectively) were imaged in regions corresponding to the superficial (SZ), mid- (MZ) and deep zones (DZ) of grade-0 (a,c,e) and grade-1 (b,d,f) cartilage. Solid arrows show examples of cells with cytoplasmic processes and broken arrows indicate examples of clusters present in various zones of cartilage. Scale bars: 25 μm.

present, L1 < 5 μm, 5 < L2 ≤ 10 μm, 10 < L3 ≤ 15 μm and L4 > 15 μm). In grade-0 cartilage overall, 17 ± 1.8% chondrocytes exhibited cytoplasmic processes, whereas there were more abnormal chondrocytes in the mid-zone than in the deep zone (Fig. 5a; $P < 0.01$). A significantly higher percentage of chondrocytes had processes in grade-1 than grade-0 cartilage, mainly due to changes in the superficial zone (Fig. 5b; 27 ± 3.0%; $P = 0.0087$). A zone-wise analysis of chondrocyte morphology revealed that in the superficial zone of grade-1 cartilage, a higher percentage (36 ± 8%) of chondrocytes had processes compared with the superficial zone of grade-0 cartilage (Fig. 5b; 16 ± 2.6%; $P = 0.0037$). Similarly, in the mid- and deep zones of grade-1 cartilage, the percentage of chondrocytes with cytoplasmic processes appeared higher (by ~ 21 and 50%, respectively) than those in grade-0 cartilage, but not to the significance level.

Average number of cytoplasmic processes/cell. In grade-0 cartilage, the average number of processes/cell (~ 1.5) was not significantly different in the three zones (Fig. 5c). In contrast, in grade-1 cartilage this was significantly higher only in the superficial zone (Fig. 5d; $P < 0.01$). The number of processes/cell was significantly higher only in the superficial zone in grade-1 compared with grade-0 cartilage (Fig. 5d; $P = 0.02$).

Length of cytoplasmic processes. In grade-0 cartilage, cytoplasmic processes in the superficial and mid-zones were ~ 4.5 μm, and significantly greater than those in the deep zone (~ 2.7 μm Fig. 5e;

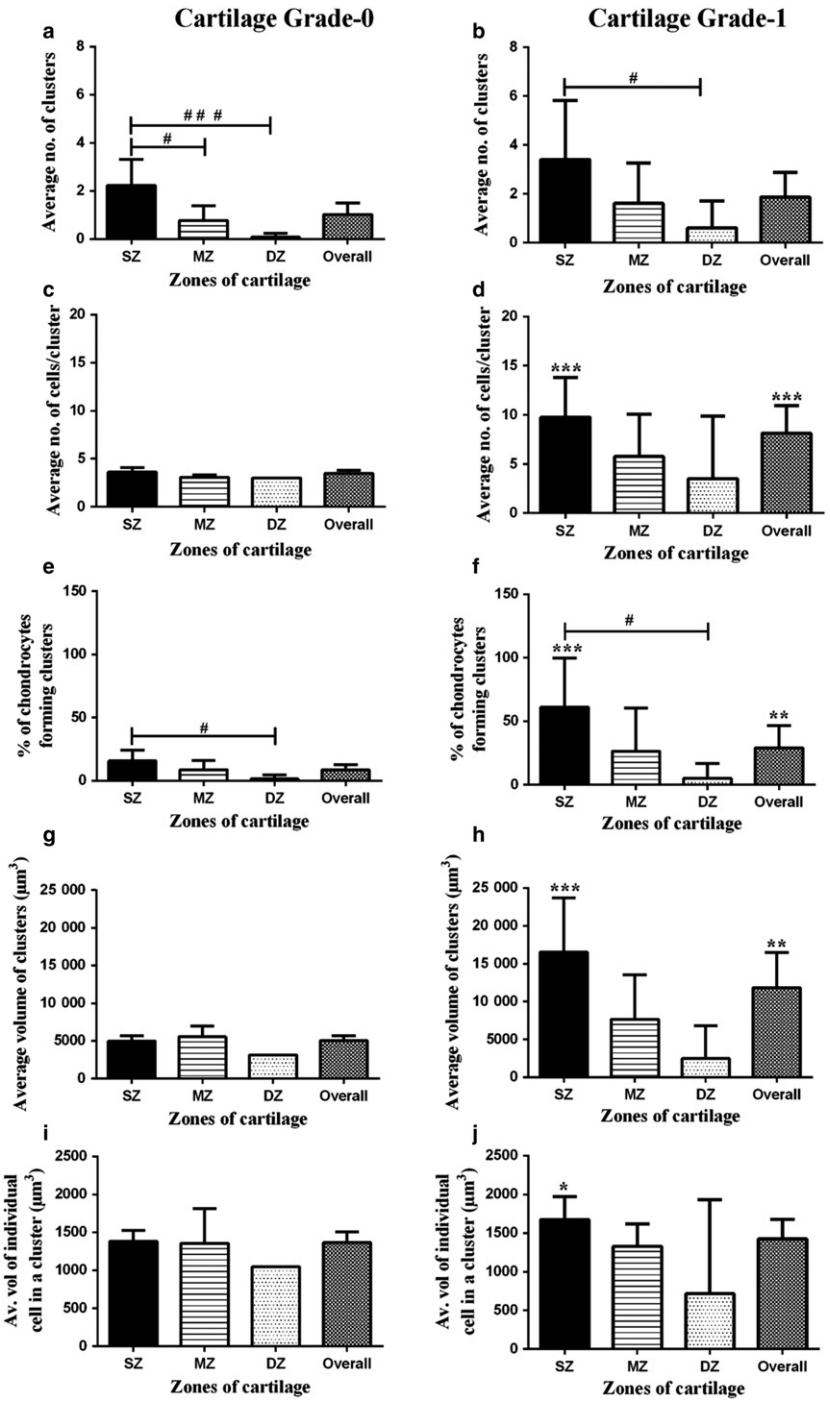

Fig. 4 Analysis of chondrocyte clusters in human femoral grade-0 and grade-1 articular cartilage. Histograms show pooled data for (a,b) average number of clusters, (c,d) average number of cells per cluster, (e,f) percentage of cells present in clusters, (g,h) average volume of clusters (μm^3) and (i,j) average volume of individual cells in a cluster (μm^3) in the superficial (SZ), mid-(MZ) and deep zones (DZ) of grade-0 and grade-1 explants. Data were from [*N(n)* = 11(1398)] for grade-0 and [*N(n)* = 5(551)] for grade-1 cartilage explants. In this and subsequent Figures, data are shown as mean ± CI (95%). A hash symbol (#) indicates a significant difference according to one-way analysis of variance followed by Tukey's multiple comparison post-hoc test. An asterisk (*) showed a significant difference between grade-0 and grade-1 cartilage explants according to an unpaired Student's *t*-test. The single, double and triple symbols showed the level of significance at $P < 0.05$, 0.01 and 0.001, respectively.

$P < 0.001$ for both). However, in grade-1 cartilage, the average length in the superficial zone (~ 14 μm) was significantly greater than those in mid-zone (~ 5 μm) and deep zone (~ 4 μm) (Fig. 5f; $P < 0.01$ for both). A comparison of average length of cytoplasmic processes in various zones of grade-0 and grade-1 cartilage, revealed significantly longer processes in the superficial and deep zone of grade-1 compared with grade-0 cartilage (Fig. 5f; $P < 0.0001$; $P = 0.03$ for superficial and deep zones, respectively). The percentage of chondrocytes with processes, the number of processes per cell and the average length of processes were all significantly higher in the superficial zone of grade-1 compared with grade-0 cartilage. This suggests that chondrocytes within the superficial zone were more likely to develop processes during cartilage degeneration.

Percentage of chondrocytes with processes of various length categories. The length of cytoplasmic processes ranged from 2 to 93 μm. To make comparisons between zones and cartilage grades, the lengths of processes were categorised into four groups and the percentage of cells having processes of a specific length category determined. In grade-0 cartilage, for all zones throughout the cartilage, a significantly higher percentage of chondrocytes had L1 processes compared with the other categories (Fig. 6a; $P < 0.001$ for overall data). In grade-1 cartilage, no differences existed between chondrocytes having cytoplasmic processes in L1–L4 categories (overall data; Fig. 6b). There was no difference between the percentage of chondrocytes having L1 processes in grade-0 and grade-1 cartilage. However, significantly higher percentages of chondrocytes had cytoplasmic processes with L2 and L3 categories in grade-1 as compared with grade-0 cartilage (Fig. 6b; $P < 0.05$ for both).

Superficial zone. In grade-0 cartilage, 11 ± 1.2% chondrocytes exhibited L1 processes, which was significantly higher than L2 (5 ± 1% cells) or L3 (1 ± 0.3%) (Fig. 6a; $P < 0.01$ and $P < 0.001$, respectively); no cells had L4 processes. In contrast, in the superficial zone of grade-1 cartilage, ~ 12% of the chondrocytes had processes within all length

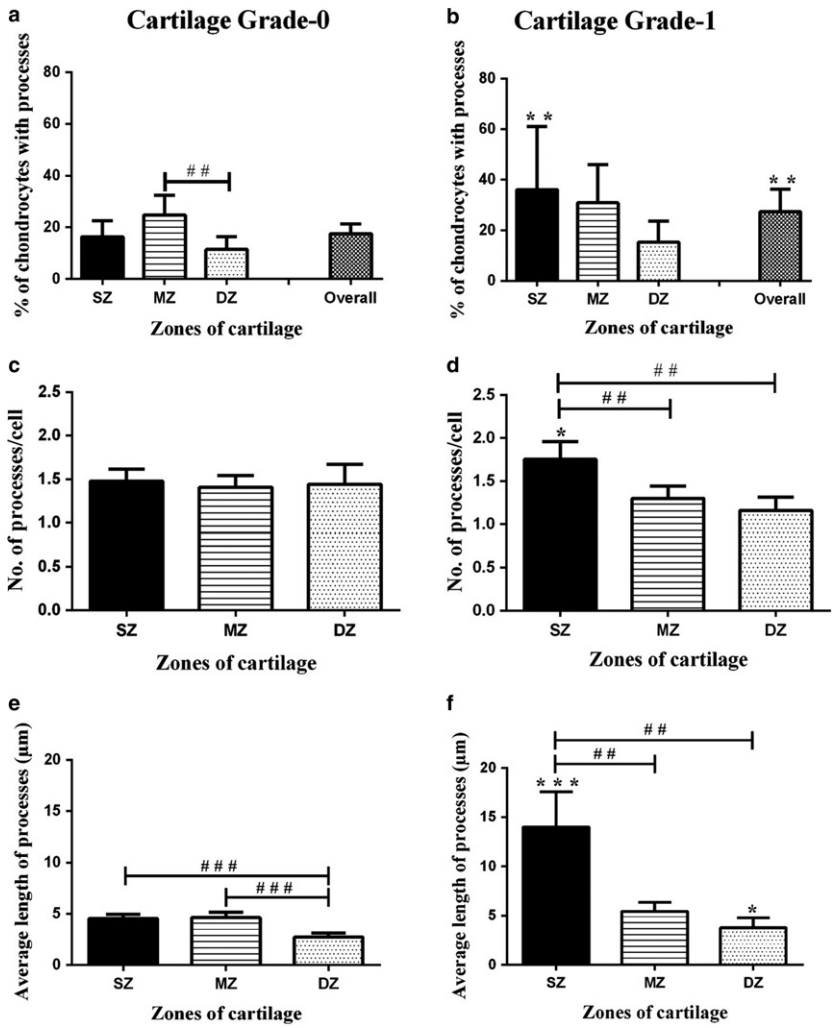

Fig. 5 Morphological characteristics of chondrocytes in grade-0 and grade-1 human femoral head articular cartilage. Histograms show pooled data regarding (a,b) percentage of cells with cytoplasmic processes, (c,d) number of processes per cell and (e,f) average length of cytoplasmic processes (μm) in the superficial (SZ), mid-(MZ) and deep zones (DZ) of grade-0 and grade-1 cartilage. Data (mean ± 95% CI) were from *N(n)* = 11 (1398) and *N(n)* = 5(551) for grade-0 and grade-1 cartilage explants, respectively. A hash symbol (#) indicates a significant difference according to one-way analysis of variance followed by Tukey's multiple comparison post-hoc test. An asterisk (*) showed a significant difference between grade-0 and grade-1 cartilage explants according to Student's *t*-test. The single, double and triple symbols showed the level of significance for $P < 0.05$, 0.01 and 0.001, respectively.

categories compared with grade-0 cartilage, with no significant difference between percentages of chondrocytes in each length category (Fig. 6b; $P > 0.05$). When the percentage of superficial zone chondrocytes with processes of various length categories were compared between grade-0 and grade-1, no difference existed with the L1 category, whereas a significantly higher percentage of chondrocytes had processes in L2, L3 and L4 (Fig. 6b; $P = 0.04$, $P = 0.03$ and $P = 0.04$, respectively). Therefore, the percentage of chondrocytes having processes with L2–L4 categories increased in the superficial zone of grade-1 compared to grade-0 cartilage (Fig. 6b).

Mid-zone. In grade-0 and grade-1 cartilage, the length of processes ranged from L1 to L3, with no processes in L4. In both grade-0 and grade-1, a significantly higher percentage of chondrocytes had processes in the L1 category compared with L2 and L3 (Fig. 6a,b; $P < 0.01$). When the mid-zone of grade-0 and grade-1 cartilage was compared, no significant difference existed between percentages of cells with processes in L1–L3 length categories. These results suggested that no difference existed between the percentages of chondrocytes with cytoplasmic processes of various lengths in the mid-zone of grade-1 compared with grade-0 cartilage.

Deep zone: In grade-0 cartilage, only L1 processes were observed. Chondrocytes with L1 and L2 were present in grade-1, whereas processes in L3 and L4 categories were absent. In grade-1 cartilage, a significantly higher percentage of chondrocytes had processes in the L1 than in the L2 category (Fig. 6b; $P < 0.001$). When the deep zones of grade-0 and grade-1 cartilage were compared, there was no significant difference between the percentages of chondrocytes in the L1 category ($P > 0.05$). However, a significantly higher percentage of chondrocytes had processes with L2 category in grade-1 than grade-0 cartilage (Fig. 6b; $P = 0.0019$). Throughout the cartilage, there existed no difference regarding the presence of L1 processes, but a significantly higher percentage of chondrocytes had processes of L2 and L3 categories in grade-1 than grade-0 cartilage (Fig. 6b; $P = 0.0078$ and $P = 0.039$, respectively). Thus, with cartilage degeneration, the percentage of chondrocytes with abnormal morphology, with the number of processes/cell and the average length of cytoplasmic processes increased, and these changes were most pronounced in the superficial zone. When L0 chondrocytes (i.e. those with 'normal' morphology – no cytoplasmic processes) in all zones were compared, overall there was a significant decrease ($P = 0.015$) between grade-0 and grade-1 cartilage (Fig. 6a,b).

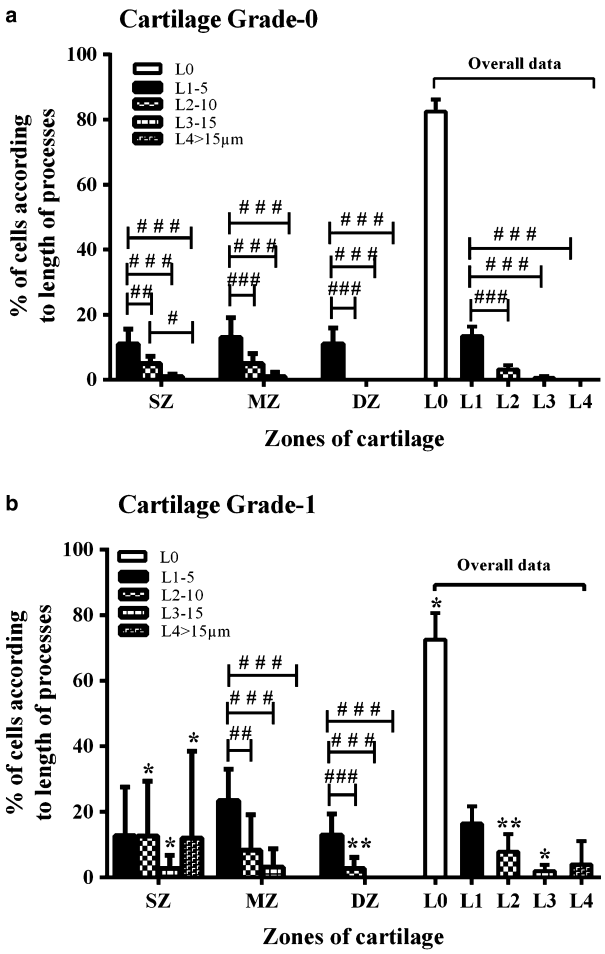

Fig. 6 Abnormal chondrocyte morphology with cartilage depth and grade. Histograms show pooled data for the percentage of chondrocytes with cytoplasmic processes of various lengths in the superficial (SZ), mid-(MZ) and deep zones (DZ) of (a) grade-0 and (b) grade-1 human femoral head articular cartilage. Data (mean ± 95% CI) were from *N(n)* = 11(1398) and *N(n)* 5(551) for grade-0 and grade-1 cartilage explants, respectively. A hash symbol (#) indicates a significant difference according to one-way analysis of variance followed by Tukey's multiple comparison post-hoc test. An asterisk (*) showed a significant difference between grade-0 and grade-1 cartilage explants according to Student's *t*-test. The single, double and triple symbols showed the level of significance for $P < 0.05$, 0.01 and 0.001, respectively.

Discussion

Confocal laser scanning microscopy and quantitative imaging identified features of *in situ* chondrocytes in normal (grade-0, non-degenerate) and grade-1 (mildly degenerate) human femoral head articular cartilage. While some classical aspects of chondrocytes previously reported using standard histological methods were clearly evident (e.g. clustering), the methods used here provided quantifiable data which revealed marked changes to chondrocyte clustering and fine cell morphology between grade-0 and grade-1 cartilage. This allowed a deeper insight into the

micro-anatomical properties of normal human cartilage and some of the changes evident with cartilage degeneration than have been obtained to date.

Accurate cartilage grading is essential to ensure that grade-0 and grade-1 cartilage are clearly and reproducibly defined. In addition to the standard criteria (Pritzker et al. 2006), confocal laser scanning microscope imaging of the surface was invaluable, as grade-0 cartilage appeared 'smooth', whereas grade-1 cartilage was uneven, allowing discrimination between these grades (Fig. 1c,d). Careful cartilage grading permitted areas of grade-0 and grade-1 tissue to be studied because of the focal nature of osteoarthritis (e.g. in femoral condyle (Squires et al. 2003; Rolauffs et al. 2010)) or tibial plateau (Squires et al. 2003). In the superficial zone of grade-0 cartilage, chondrocyte clusters were occasionally observed (Figs 3 and 4) and this has also been reported in relatively non-degenerate (grade-0 and grade-1) cartilage obtained from other joints, e.g. distal femur (condyles, patellofemoral groove) and proximal tibia (Rolauffs et al. 2010). However, in grade-1 cartilage, clustering increased with the average number of clusters throughout the cartilage, the average number of cells/cluster and the percentage of cells forming clusters, particularly in the superficial zone, increasing significantly (Fig. 4a-f). The total volume of clusters and the number of chondrocytes/cluster suggested that the increase in cluster size was due to chondrocyte proliferation rather than swelling/hypertrophy, as there was only a small increase in superficial zone chondrocyte size (~ 20%) but the volume of clusters increased more than threefold (Fig. 4g–h). This supports previous studies indicating that in human osteoarthritis, cartilage cell proliferation was the principal mechanism for cluster formation (Lotz et al. 2010). The nature of the peri-cellular matrix (lacuna) surrounding chondrocyte clusters is of interest and could be observed in some confocal images by adjusting the brightness and contrast. Preliminary studies suggested that the lacuna encapsulated the whole cell cluster and that individual lacunae appeared to merge into one large 'bag' surrounding the cell cluster (A. Karim, unpublished).

The majority of chondrocytes within femoral head cartilage were morphologically 'normal' (approximately 80%); however, there was a significant decrease from grade-0 and grade-1 (Fig. 6a,b). Despite this, confocal laser scanning microscope imaging of fluorescently labelled chondrocytes revealed that 15–25% exhibited at least one cytoplasmic process of ~ 5 μm in length (Fig. 5a). These processes were unlikely to be due to cutting damage during sampling because abnormal cell morphology was also observed in axial views (Fig. 2) where cells were visualised distant from any cut edge. With degeneration to grade-1, marked changes to chondrocyte morphology occurred and there were increases in the percentage of chondrocytes with processes and the length of processes, particularly for cells in the superficial zone (Fig. 5). We should note that the present results relate only to small areas of the cartilage available and it may be premature to assume that the changes reported here are uniform over the whole cartilage surface of the femoral head. Although we compared cartilage from four different regions of the femoral head (parafoveal anterior, parafoveal posterior, parafoveal superior and parafoveal inferior) and found no obvious difference regarding percentage of cells with cytoplasmic processes and the length of these processes, it is quite likely that on a microscopic scale, there is marked heterogeneity in both chondrocyte morphology and extracellular matrix composition.

At present, we do not have a clear explanation for the development of these cytoplasmic processes. They may form 'passively', e.g. from loss/damage to the surrounding pericellular matrix, perhaps related to the older donors we studied and aged cartilage, which is known to be associated with a reduced size/content of matrix proteoglycans (Dudhia, 2005). However, a previous study on tibial plateau grade-0 cartilage obtained from total knee replacement operations, albeit from a relatively small number of patients ($N = 21$) and age range (49–86 years), did not find a relation between the percentage of normal chondrocytes and patient age (Murray et al. 2010). Disruption to pericellular collagen Type VI may also be involved (Guilak et al. 2006; Murray et al. 2010), as its depletion around chondrocytes could provide a weak area into which process(es) could develop. For example, chondrocytes cultured in soft, as opposed to stiff, agarose gels produce cytoplasmic processes with similar structures to those described in the present study (Karim & Hall, 2017). Alternatively, the development of processes could result from mechanically injured chondrocytes leading to an 'active' metabolic response and resulting in the release of cytokines/degradative enzymes and breakdown of the pericellular matrix. It is possible that both 'active' and 'passive' responses are responsible. It is notable that similar chondrocyte cytoplasmic processes of chondrocytes develop in mechanically (scalpel) injured bovine articular cartilage, but only when fetal calf serum is present (Karim & Hall, 2016). It is possible that the penetration of proliferative factors (e.g. fibroblast growth factor) from the synovial fluid (Quintavalla et al. 2005; Karim & Hall, 2016) through a weakened matrix could actively initiate changes in chondrocyte morphology.

There is a close relationship between chondrocyte shape and matrix metabolism (Von der Mark et al. 1977; Cancedda et al. 1995). Chondrocyte de-differentiation to a fibroblastic-like phenotype which is characterised by cytoplasmic processes, reduces synthesis/release of cartilage-specific components, e.g. collagen Type II, aggrecan, and increases collagen Type I and small proteoglycan production (Stokes et al. 2002). Changes in chondrocyte shape also stimulate levels of agents implicated in extracellular matrix breakdown (Page-McCaw et al. 2007), leading to a localised matrix loss (Hollander et al. 1995) and potentially further increasing the development of cytoplasmic processes. A central role for transforming growth factor β1-induced

signalling in human osteoarthritis has been reported, which may promote a fibroblastic phenotype (Plaas et al. 2011). The presence of abnormal and/or clustered chondrocytes, with compromised matrix metabolism in otherwise non-degenerate (grade-0) cartilage, could indicate an early weakening in the association between chondrocytes and surrounding peri-cellular matrix, and increase vulnerability to mechanical loading (Alexopoulos et al. 2005). This could raise the possibility of chondrocyte injury/death, increasing the risk of cartilage degeneration (Hashimoto et al. 1998; Del Carlo & Loeser, 2008). It would be of particular interest to determine the influence of the morphological changes reported here on the cytoskeletal structure of *in situ* chondrocytes, matrix metabolism and the structure/composition of the pericellular and bulk extracellular matrix.

These results suggested that even in apparently normal, non-degenerate cartilage, the spatial organisation (clustering) and morphology (cytoplasmic processes) of chondrocytes is altered from that classically described in the literature. It is known that a change in chondrocyte morphology indicates the loss of phenotype associated with the maintenance of a cartilage-specific and resilient extracellular matrix capable of withstanding mechanical load (Aigner et al. 2007). The presence in otherwise normal cartilage of a relatively small population of chondrocytes as clusters and/or with morphological abnormalities could reflect local physico-chemical conditions, cartilage age or pericellular matrix integrity. The present results demonstrating increased chondrocyte clustering and morphological abnormalities with cartilage degeneration, identified aberrant chondrocytes that potentially are producing a defective and weakened extracellular matrix.

Acknowledgements

This study was funded by the University of Health Sciences, Lahore and Higher Education Commission, Pakistan, and the College of Medicine and Veterinary Medicine, University of Edinburgh. We thank Dr A. Kubasik-Thayil for expert assistance with the confocal scanning laser microscope. We also thank Dr P. Bush for helpful comments during this research.

Author's contributions

A.K., A.K.A., A.C.H.: conception and design. A.K., A.K.A., A.C.H.: analysis, statistical evaluation and interpretation of data. A.K, A.C.H.: drafting of the manuscript. A.K., A.K.A., A.C.H.: critical revision of the article for important intellectual content. A.K., A.K.A., A.C.H.: final approval of the manuscript.

Conflict of interest

The authors do not have any conflicts of interest to declare in relation to the work presented here.

References

Aigner T, Soder S, Gebhard PM, et al. (2007) Mechanisms of disease: role of chondrocytes in the pathogenesis of osteoarthritis – structure, chaos and senescence. *Nat Clin Pract Rheumatol* **3**(3), 391–399.

Alexopoulos LG, Setton LA, Guilak F (2005) The biomechanical role of the pericellular matrix in articular cartilage. *Acta Biomater* **1**, 317–325.

Amin AK, Bush PG, Huntley JS, et al. (2008) Osmolarity influences chondrocyte death in wounded articular cartilage. *J Bone Joint Surg* **90**, 1531–1542.

Aydelotte MB, Kuettner KE (1988) Differences between subpopulations of cultured bovine articular chondrocytes. I. Morphology and cartilage matrix production. *Conn Tiss Res* **18**, 205–222.

Benya PD, Shaffer JD (1982) Dedifferentiated chondrocytes reexpress the differentiated collagen phenotype when cultured in agarose gels. *Cell* **30**, 215–224.

Blaine EJ (2009) Involvement of the cytoskeletal elements in articular cartilage homeostasis and pathology. *Int J Exp Pathol* **90**, 1–15.

Buckwalter JA, Mankin HJ (1997) Articular cartilage. Part II. Degeneration and osteoarthrosis, repair, regeneration and transplantation. *J Bone Joint Surg* **79**, 612–632.

Bush PG, Hall AC (2001) The osmotic sensitivity of isolated and *in situ* bovine articular chondrocytes. *J Orthop Res* **19**, 768–778.

Bush PG, Hall AC (2003) The volume and morphology of chondrocytes within non-degenerate and degenerate human articular cartilage. *Osteoarthritis Cartilage* **11**, 242–251.

Cancedda R, Descalzi-Cancedda F, Castagnola P (1995) Chondrocyte differentiation. *Int Rev Cytol* **59**, 265–358.

Chen SS, Falcovitz YH, Schneiderman R, et al. (2001) Depth-dependent compressive properties of normal aged human femoral head articular cartilage: relationship to fixed charge density. *Osteoarthritis Cartilage* **9**, 561–569.

Del Carlo M Jr, Loeser RF (2008) Cell death in osteoarthritis. *Curr Rheumatol Rep* **10**, 37–42.

Dowthwaite GP, Bishop JC, Redman SN, et al. (2004) The surface of articular cartilage contains a progenitor cell population. *J Cell Sci* **117**, 889–897.

Dudhia J (2005) Aggrecan, aging and assembly in articular cartilage. *Cell Mol Life Sci* **62**, 2241–2256.

Grodzinsky AJ, Levenston ME, Jin M, et al. (2000) Cartilage tissue remodelling in response to mechanical forces. *Annu Rev Biomed Eng* **2**, 691–713.

Guilak F, Alexopoulos LG, Upton ML, et al. (2006) The pericellular matrix as a transducer of biomechanical and biochemical signals in articular cartilage. *Ann N Y Acad Sci* **1068**, 498–512.

Hashimoto S, Ochs RJ, Komiya S, et al. (1998) Linkage of chondrocyte apoptosis and cartilage degeneration in human osteoarthritis. *Arthritis Rheum* **41**, 1632–1638.

Hembree WC, Ward BD, Furman BD, et al. (2007) Viability and apoptosis of human chondrocytes in osteochondral fragments following joint trauma. *J Bone Joint Surg Br* **89**, 1388–1395.

Hollander AP, Pidoux I, Reiner A, et al. (1995) Damage to type II collagen in aging and osteoarthritis starts at the articular surface, originates around chondrocytes, and extends into the cartilage with progressive degeneration. *J Clin Invest* **96**, 2859–2869.

Holloway I, Kayser M, Lee DA, et al. (2004) Increased presence of cells with multiple elongated processes in osteoarthritic femoral head cartilage. *Osteoarthritis Cartilage* **12**, 17–24.

Huntley JS, Simpson AH, Hall AC (2005) Use of non-degenerate human osteochondral tissue and confocal laser scanning microscopy for the study of chondrocyte death at cartilage surgery. *Eur Cell Mater* **9**, 13–22.

Hunziker EB (1992) Articular cartilage structure in humans and experimental animals. In: *Articular Cartilage and Osteoarthritis* (eds Kuettner KE, Schleyerbach R, Peyron JG, Hascall VC), pp. 183–199. New York: Raven Press.

Karim A, Hall AC (2016) Hyperosmolarity normalizes serum-induced changes to chondrocyte properties in a model of cartilage injury. *Eur Cell Mater* **31**, 205–220.

Karim A, Hall AC (2017) Chondrocyte morphology in stiff and soft agarose gels and the influence of fetal calf serum. *J Cell Physiol* **232**, 1041–1052.

Kouri JB, Arguello C, Luna J, et al. (1998) Use of microscopical techniques in the study of human chondrocytes from osteoarthritic cartilage: an overview. *Microsc Res Tech* **40**, 22–36.

Lotz MK, Otsuki S, Grogan SP, et al. (2010) Cartilage cell clusters. *Arthritis Rheum* **62**, 2206–2218.

Mallein-Gerin F, Garrone R, van der Rest M (1991) Proteoglycan and collagen synthesis are correlated with actin organisation in dedifferentiating chondrocytes. *Eur J Cell Biol* **56**, 364–373.

McGlashen SR, Cluett EC, Jensen CG, et al. (2008) Primary cilia in osteoarthritic chondrocytes: from chondrons to clusters. *Dev Dyn* **237**, 2013–2020.

Murray DH, Bush PG, Brenkel IJ, et al. (2010) Abnormal human chondrocyte morphology is related to increased levels of cell-associated IL-1β and disruption to pericellular collagen type VI. *J Orthop Res* **28**, 1507–1514.

Page-McCaw A, Ewald AJ, Werb Z (2007) Matrix metalloproteinases and the regulation of tissue remodelling. *Nat Rev Mol Cell Biol* **8**, 221–233.

Paterson SI, Amin AK, Hall AC (2015) Airflow accelerates bovine and human articular cartilage drying and chondrocyte death. *Osteoarthritis Cartilage* **23**, 257–265.

Plaas A, Velasco J, Gorski DJ, et al. (2011) The relationship between fibrogenic TGFβ1 signalling in the joint and cartilage degradation in post-injury osteoarthritis. *Osteoarthritis Cartilage* **19**, 1081–1090.

Poole CA, Matsuoka A, Schofield JR (1991) Chondrons from articular cartilage. III Morphologic changes in the cellular microenvironment of chondrons isolated from osteoarthritic cartilage. *Arthritis Rheum* **34**(1), 22–35.

Pritzker KPH, Gay S, Jimenez SA, et al. (2006) Osteoarthritis cartilage histopathology: grading and staging. *Osteoarthritis Cartilage* **13**, 13–29.

Quintavalla J, Kumar C, Daouti S, et al. (2005) Chondrocyte cluster formation in agarose cultures as a functional assay to identify genes expressed in osteoarthritis. *J Cell Physiol* **204**, 560–566.

Rolauffs B, Williams JM, Aurich M, et al. (2010) Proliferative remodelling of the spatial organisation of human superficial chondrocytes distant to focal early osteoarthritis (OA). *Arthritis Rheum* **62**(2), 489–498.

Rothwell AG, Bentley G (1973) Chondrocyte multiplication in osteoarthritic articular cartilage. *J Bone Joint Surg Br* **55**, 588–594.

Rottmar M, Mhanna R, Guimond-Lischer S, et al. (2014) Interference with the contractile machinery of the fibroblastic chondrocyte cytoskeleton induces re-expression of the cartilage phenotype through involvement of PI3K, PKC and MAPKs. *Exp Cell Res* **320**, 175–187.

Schumacher BL, Su JL, Lindley KM, et al. (2002) Horizontally oriented clusters of multiple chondrons in the superficial zone of ankle, but not knee articular cartilage. *Anat Rec* **266**, 241–248.

Shibakawa A, Aoki H, Masuko-Hongo K, et al. (2003) Presence of pannus-like tissue on osteoarthritic cartilage and its histological character. *Osteoarthritis Cartilage* **11**, 133–140.

Simpkin V, Murray DH, Hall AP, et al. (2007) Bicarbonate-dependent pH_i regulation by chondrocytes within the superficial zone of bovine articular cartilage. *J Cell Physiol* **212**, 600–609.

Squires GR, Okouneff S, Ionescu M, et al. (2003) The pathobiology of focal development in aging human articular cartilage and molecular matrix changes characteristic of osteoarthritis. *Arthritis Rheum* **48**, 1261–1270.

Stokes DG, Liu G, Dharmavaram R, et al. (2001) Regulation of type-II collagen gene expression during human chondrocyte de-differentiation and recovery of chondrocyte-specific phenotype in culture involves Sry-type high-mobility-group box (SOX) transcription factors. *Biochem J* **360**, 461–470.

Stokes DG, Liu G, Coimbra IB, et al. (2002) Assessment of the gene expression profile of differentiated and dedifferentiated human fetal chondrocytes by microarray analysis. *Arthritis Rheum* **46**, 404–419.

Tesche F, Miosge N (2005) New aspects of the pathogenesis of osteoarthritis: the role of fibroblast-like chondrocytes in late stages of the disease. *Histol Histopathol* **20**, 329–337.

Vanderploeg EJ, Wilson CG, Levenston ME (2008) Articular chondrocytes derived from distinct tissue zones differentially respond to *in vitro* oscillatory tensile loading. *Osteoarthritis Cartilage* **16**, 1228–1236.

Von der Mark JK, Gauss V, von der Mark H, et al. (1977) Relationship between cell shape and type of collagen synthesised as chondrocytes lose their cartilage phenotype in culture. *Nature* **267**, 531–532.

Wong M, Wuethrich P, Eggli P, et al. (1996) Zone-specific cell biosynthetic activity in mature bovine articular cartilage: a new method using confocal microscopic stereology and quantitative autoradiography. *J Orthop Res* **14**, 424–432.

Woods A, Wang G, Beier F (2007) Regulation of chondrocyte differentiation by the actin cytoskeleton and adhesive interactions. *J Cell Physiol* **213**, 1–8.